# Micellization of Telechelic Associative Polymers: Self-Consistent Field Modeling and Comparison with Scaling Concepts

**ARTICLE** *in* THE JOURNAL OF PHYSICAL CHEMISTRY B · APRIL 2007

Impact Factor: 3.3 · DOI: 10.1021/jp0683768 · Source: PubMed



**4 AUTHORS**, INCLUDING:

Joris Sprakel
Wageningen University
**78** PUBLICATIONS **853** CITATIONS

SEE PROFILE

Nicolaas A M Besseling
Delft University of Technology
**91** PUBLICATIONS **1,710** CITATIONS

SEE PROFILE

Frans A M Leermakers
Wageningen University
**288** PUBLICATIONS **4,744** CITATIONS

SEE PROFILE

# Micellization of Telechelic Associative Polymers: Self-Consistent Field Modeling and Comparison with Scaling Concepts

**J. Sprakel,*,†,‡ N. A. M. Besseling,† F. A. M. Leermakers,† and M. A. Cohen Stuart†**

*Laboratory of Physical Chemistry and Colloid Science, Wageningen University, Dreijenplein 6, 6703 HB, Wageningen, The Netherlands, and Dutch Polymer Institute (DPI), P.O. Box 902, 5600 AX Eindhoven, The Netherlands*

*Received: December 6, 2006; In Final Form: January 11, 2007*

We present numerical results from self-consistent field calculations on the micellization of telechelic associative polymers and their mono-functional analogues. These results are confronted with relatively simple scaling concepts. The proportionality of the critical micelle concentration (CMC) with the hydrophilic backbone length, as found in the calculations, shows good correspondence with a scaling argument based on the entropic penalty of loop formation. It is also shown that models for the conformation of spherical brushes can be applied to predict the structure of the flowerlike micelles formed by these telechelic polymers. Furthermore, we find good agreement between the numerical dependence of the aggregation number upon both backbone and terminal hydrophobe length and an analytical expression derived from the well-known Daoud−Cotton model by introducing a correction for the finite size of the micellar core.

## Introduction

Telechelic associative polymers are lyophilic polymer chains end-capped with lyophobic moieties. A well-known class of associative polymers are so-called HEURs or hydrophobically modified ethoxylated urethanes, which are poly(ethylene oxide)s with paraffinic tails grafted at both ends of the chain. They are analogues of simple nonionic surfactants.

In a polar solvent, at concentrations above the critical micelle concentration (CMC), these telechelics self-assemble into spherical, flowerlike micelles. At higher concentrations, above a percolation threshold, they form transient, micellar networks.[1] Some of the polymers in this class have been reported to show an entropically driven demixing into a dilute (micellar) phase and a condensed phase with a higher polymer concentration (typically 1 wt %).[2]

For a better understanding of the phase behavior of these associative polymers, which is of practical importance in the formulation of, e.g., paints and inks, we first study their micellization in detail.

Some crude analytical models for the properties of telechelic micelles have been reported.[3,4] Francois et al.[4] apply the scaling concepts of Halperin and Alexander[5,6] to explain experimental neutron scattering data. However, they neglect the loop entropy contribution to the free energy of these micelles, leading to underestimation of the CMC. The large influence of this entropic penalty associated with loop formation on the micellization of telechelics was first stressed by Ten Brinke and Hadziioannou[7] and further elaborated by, e.g., Balsara et al.[8]

In order to predict aggregation numbers for telechelic micelles, Meng and Russel[9] balanced the interfacial and configurational free energy of the micellar core chains against the elastic stretching of the coronal chains. To account for the latter, they use a model by Li and Witten[10] that was published earlier by Wijmans and Zhulina.[11] In these models for the conformation of spherical brushes, two zones are predicted; in the inner zone, closest to the core, the density decay of the chains is predicted to show power-law behavior, after which (outer zone) the density follows a parabolic profile. This parabolic density profile, for curved polymer brushes, was first observed by Dan and Tirrel in numerical self-consistent field calculations.[12] The power-law behavior close to the core was predicted by Daoud and Cotton in their model for the conformations of star-shaped polymers.[13]

We use the discrete self-consistent field theory of Scheutjens and Fleer[14] to study the properties of isolated micelles assembled from telechelic chains, adopting a molecular model that has been shown effective in predicting the micellization of nonionic surfactants[15] and block copolymers.[16] The numerical results are confronted with approximate, yet insightful, scaling arguments, where our main focus is on the dependencies of the CMC and the aggregation number upon the molecular architecture.

**Thermodynamics and SCF Modeling.** To study the micellization of telechelic polymers, we start from the thermodynamics of small systems, as described in the classical work of Hill[17] and Hall and Pethica.[18] For micellar systems, the classical expression for the change of the internal energy $U$ of a macroscopic system, with a change in entropy $S$, volume of the system $V$, and/or the numbers of molecules $n_i$ of each component $i$, is extended with an additional term to account for the energy stored in the micelles:

$$\mathrm{d}U = T\,\mathrm{d}S - P\,\mathrm{d}V + \sum_i \mu_i\,\mathrm{d}n_i + \epsilon\,\mathrm{d}\mathcal{N} \qquad (1)$$

with $\epsilon$ being the subdivision potential, easily identified as the grand potential ($\Omega$) per micelle, $\mathcal{N}$ the number of micelles, $P$ the pressure, $\mu$ the chemical potential, and $T$ the temperature. From the Helmholtz energy, $F = U - TS$, we can formulate two constraints

$$\left.\frac{\partial F}{\partial \mathcal{N}}\right|_{n_i,V,T} = \epsilon = 0 \qquad (2)$$

† Laboratory of Physical Chemistry and Colloid Science.
‡ Dutch Polymer Institute (DPI).

10.1021/jp0683768 CCC: $37.00 
Published on Web 02/24/2007

to ensure that the macroscopic thermodynamics are conserved, and

$$\left.\frac{\partial^2 F}{\partial \mathcal{N}^2}\right|_{n,V,T} = \left.\frac{\partial \epsilon}{\partial \mathcal{N}}\right|_{n_i,V,T} > 0 \tag{3}$$

that assures the stability of the micelles.

In the calculations, we are restricted to considering a single micellar object. To apply the constraints above, formulated for a macroscopic system of many micelles, to a single-micelle system, we use the following argument; we can consider the system with a single micelle to be a sub-system of a larger closed ensemble (constant $n_i$, $V$, $T$) of many micelles. In this system, an increase in the aggregation number $n_{agg}$, results in an equivalent decrease of the number of micelles. Now, using the grand potential per micelle $\Omega = (F/\mathcal{N}) - \sum_i \mu_i(n_i/\mathcal{N}) + p(V/\mathcal{N})$, we can write the stability constraint as

$$\left.\frac{\partial \Omega}{\partial n_{agg}}\right|_{n_i,V,T} < 0 \tag{4}$$

that will give us ground for defining the critical micelle concentration in a subsequent section of this paper.

The self-consistent field method is ideally suited to obtain information on the grand potential for micellar systems in a molecular model. In this paper, we apply a self-consistent field method using the discretization scheme of Scheutjens and Fleer.[14,19,20,21] In this method, the same length scale ($l$) is used to subdivide space into lattice sites and molecules into segments. For the sake of brevity, we will only discuss the major premises.

The first step is to make a choice for a lattice geometry, with the direct consequence that the shape of the self-assembled object is fixed. We shall consider a micelle pinned in the center of a spherical coordinate system where sites of equal volume ($l^3$) are arranged in concentric layers. The number of sites in layer $z$ is proportional to $z^2$. The mean-field approximation is applied to all sites in a layer, implying that inhomogeneities are allowed in the radial direction only. The radial distance from the center of the lattice is $z$. Segments, with rank number $s = 1...N$, are placed on the lattice as step-weighted walks, giving freely jointed chains in a self-consistent potential field. In effect, in a self-consistent field model, there exists a pair of conjugated functions per segment type $j$; the volume fraction profiles $\varphi_j(z)$ and the corresponding segment potential profiles $u_j(z)$. In the potentials, there are contributions of packing and nearest-neighbor interactions, accounted for by Flory−Huggins interaction parameters.

The probability of finding a molecule $i$ in a conformation $c$ is proportional to the Boltzmann weight $p = \exp(-u_i^c/k_BT)$ of the corresponding segment potential $u_i^c = \sum_s u(z_{s,i}^c)$, where $z_{s,i}^c$ is the coordinate of segment $s$ of molecule $i$ in conformation $c$. The volume fraction profiles $\varphi_i(z)$ of all species $i$ are found after normalization of the sum of the Boltzmann weights of all possible conformations. The self-consistent field equations are satisfied when the segment potentials and volume fractions are consistent, meaning that the potentials of both determine and follow from the volume fractions. This solution is obtained by a numerical iteration procedure. The correct solution obeys the incompressibility constraint: $\sum_i \varphi_i(z) = 1\ \forall z$.

When a consistent solution for the volume fractions and potentials is found, the grand potential for a single micelle $\Omega(\{\varphi_i(z)\},\{u_i(z)\})$, which is a functional of the profiles $\varphi_i(z)$ and $u_i(z)$, can be calculated. It can be interpreted as the translationally restricted subdivision potential, because we neglect the translational entropy of the entire micellar object that is pinned in the center of the lattice. In this paper, we will focus on the most probable micelle, but in this same method, it is possible to obtain information on the size distribution of micelles through analysis of the fluctuations in the aggregation number.[22]

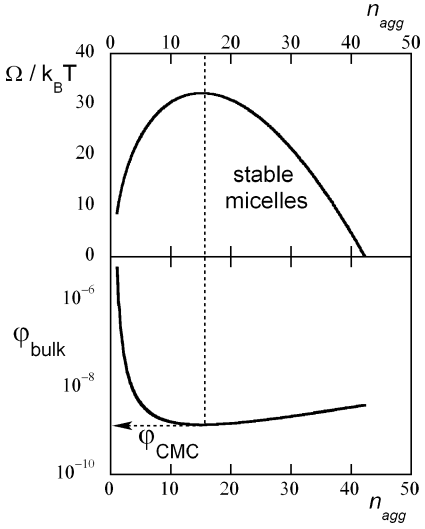


**Figure 1.** Grand potential $\Omega$ and polymer bulk volume fraction $\varphi_{bulk}$ versus aggregation number $n_{agg}$ for a $C_{20}EO_{200}C_{20}$ micellar system in a $\theta$ solvent ($\tau = 0$).

We model the telechelic associative polymers of the HEUR type using two types of segments, labeled C, which stands for $CH_2$ or $CH_3$, and O. Their general structure is $C_{N_T}(CCO)_{N_{EO}}C_{N_T}$, where CCO represents an ethylene oxide (EO) monomer and $C_{NT}$ is an aliphatic tail. Their mono-functional analogues are given by $C_{NT}(CCO)_{(1/2)N_{EO}}$. Because the polymers are modeled as freely jointed chains, the Kuhn length equals 1 segment. Hence, the number of Kuhn segments in a polymer backbone $N_B$ is $3N_{EO}$. A solvent molecule takes five lattice sites ($N_S = 5$); it consists of a central segment connected to four neighbors, all of type W.

The various interactions can be tuned with the Flory−Huggins interaction parameters ($\chi$) between the different segments.[23] The hydrophobic interaction between the tails, which drives the micellization, is set by $\chi_{CW}$; in these calculations, $\chi_{CW}$ is constant at a value of 1.1. $\chi_{CO}$ is set at 2, which supresses the solubility of the polymeric backbone in the hydrophobic core of the micelle. The solvency of the EO-backbone can be tuned with $\chi_{OW}$. The effective interaction parameter for an averaged backbone segment with the solvent can be calculated with

$$\chi_{BW} = \chi_{CWC}\mathcal{F}_C + \chi_{OW}\mathcal{F}_O - \chi_{CO}\mathcal{F}_C\mathcal{F}_O \tag{5}$$

where $\mathcal{F}_C = 2/3$ and $\mathcal{F}_O = 1/3$ are the fractions of C and O segments in the backbone, respectively. For chains in a non-monomeric solvent, we can define the Edwards excluded volume parameter $\tau$ for the polymer backbone as

$$\tau \equiv 1 - 2\chi_{BW}N_S \tag{6}$$

From eqs 5 and 6 and the choices mentioned for $\chi_{CW}$ and $\chi_{CO}$, we find that $\chi_{OW}$ needs to be set at $-0.57$ to reach $\theta$ conditions for the polymer backbone ($\tau = 0$). A more negative value for $\chi_{OW}$ will increase the solvent quality ($\tau > 0$).

This combination of molecular modeling and the accompanying values for the interaction parameters has been proven to be successful in modeling the micellization of, e.g., non-ionic surfactants[15] and block copolymers.[16]

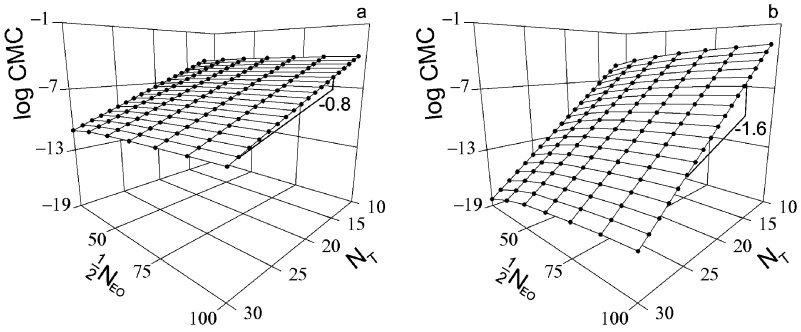


**Figure 2.** Dimensionless critical micelle number concentrations for (a) a mono-functional polymeric surfactant of type $C_{N_T}EO_{(1/2)N_{EO}}$ where CMC $= \varphi^{CMC}/((3/2)N_{EO} + N_T)$ and (b) a telechelic associative polymer of type $C_{N_T}EO_{N_{EO}}C_{N_T}$ where CMC $= \varphi^{CMC}/(3N_{EO} + 2N_T)$ under $\theta$ conditions for the backbone ($\tau = 0$).

## Results and Discussion

**CMC.** There are various ways to define the critical micelle concentration in these SF−SCF calculations. The most straightforward definition of the CMC is the polymer concentration where a first stable micelle appears. In Figure 1, a typical result from the SF−SCF calculations is shown. We calculate these quantities for a single micelle, which we consider as one subsystem of a larger ensemble of equal cells ($n_i$, $V$, $T$ constant). An increase in aggregation number inherently results in a decrease in the number of micelles in the ensemble. This justifies using the stability constraint in eq 4 for defining the CMC.

At low aggregation numbers, we first enter an unstable regime, where the system does not yet obey the stability constraint of eq 4. At a given aggregation number, the quantity $\partial\Omega/\partial n_{agg}$ will be zero, which can be regarded as the condition where the first stable micelle is formed. The unimer bulk concentration where this occurs will be our definition for the CMC.[24] Experimental CMCs will obviously be higher than this thermodynamic criterion for the CMC, as experimental methods are not sensitive enough to measure a single micelle. The experimental CMC is found when the number of micelles is significantly large, depending on the method. In fact, the scaling behavior of the CMC or the aggregation number is independent of the criterion chosen for the CMC, as long as the latter is unambiguously defined.

In Figure 2, we see the dependence of the CMC, under $\theta$ conditions for the polymer backbone ($\tau = 0$), on both the hydrophobic tail length length $N_T$ and the hydrophilic backbone length $N_{EO}$ for mono-functional chains (Figure 2a) and telechelics (Figure 2b). The CMC is given as a dimensionless number concentration, a number of molecules per lattice unit volume ($l^3$).

The exponential decay of the CMC with hydrophobe size, known as Traube's rule,[25] for the mono-functional chains obtained to be CMC $\propto \exp(-0.8N_T)$, is in good agreement with what is experimentally found for simple nonionic surfactants.[26]

It is known that the CMC is proportional to $\exp(F^m/k_BT)$, where $F^m$ is the free energy change associated with transfer of a unimer from solution into a micelle. Note that $F^m < 0$ for a stable micelle. A telechelic unimer that transfers from solution into a micelle gains twice as much interaction energy compared to the mono-functional unimer, and it loses the same amount of translational entropy. This leads to an exponential decay of the CMC with $N_T$ that is twice as strong as compared to the mono-functional associating polymers (Figure 2b). Hence, for the telechelic polymers we find that CMC $\propto \exp(-1.6N_T)$.

Figure 3 takes a closer look at the scaling of the CMC with $N_B$. Ten Brinke[7] was the first to argue that the entropic penalty due to loop formation, as predicted by Jacobson and Stockmayer

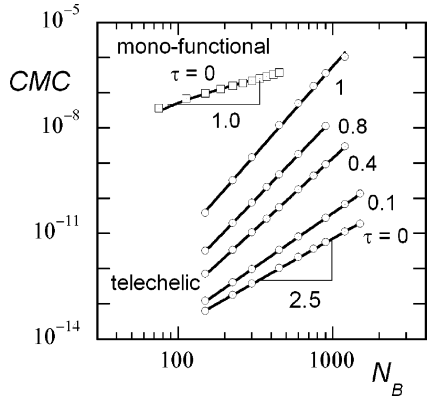


**Figure 3.** Dependence of the CMC upon the number of Kuhn segments in the backbone $N_B = 3N_{EO}$, as a function of the solvent quality, for a system of $C_{20}EO_{N_{EO}}C_{20}$ chains and a mono-functional analogue $C_{20}EO_{(1/2)N_{EO}}$.

for single Gaussian chains,[27] has a strong effect on the micellization of loop-forming polymers.

The free energy increase (i.e., entropy loss) due to loop formation, $F^{loop}$, for a micelle composed of $n_{agg}$ chains, with backbones of $N_B$ Kuhn segments long, is given by

$$F^{loop} = \frac{3}{2}\beta n_{agg} k_B T \ln N_B \tag{7}$$

where the factor $(3/2)k_BT \ln N_B$ originates from the decrease in possible conformations of a single Gaussian chain when it is required to loop back to its origin.[27] $\beta$ is a parameter accounting for nonideality of the chains. Under $\theta$ conditions, $\beta$ should be unity, and eq 7 returns to the Gaussian limit. For the CMC of telechelic chains, we can derive that

$$\mathrm{CMC} \propto \exp\left(\frac{F^m + F^{loop}}{k_B T}\right) \tag{8}$$

where CMC $= \varphi^{CMC}/(3N_{EO} + 2N_T)$ is the dimensionless critical micelle number concentration for telechelic chains and here $F^m$ is, in analogy with the mono-functional case, the free energy change associated with transfer of a telechelic unimer into a micelle, without the contribution of the formation of loops.

From the calculations, we find that for mono-functional chains CMC $\propto N_B^k$, where $k$ is an exponent that ranges from 0.9 to 1.8 depedending on $N_T$ yet independent of the solvent quality in the range considered here ($0 < \tau < 1$). The $N_T$ dependence of the exponent $k$ is possibly linked to the complicated depedence of the aggregation number on $N_T$ and $N_B$, as will be shown in a later section. Figure 3 shows the result for $\theta$ conditions ($\tau = 0$) and an alkyl length of 20. For these chains, we find that $k = 1.0$.

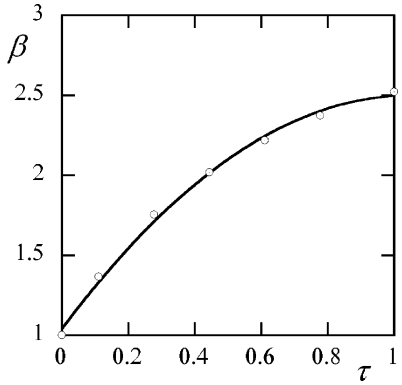


**Figure 4.** Ten Brinke's $\beta$-parameter versus the Edwards excluded volume parameter for the polymer backbone $\tau$ as found from the numerical results for $C_{20}EO_{N_{EO}}C_{20}$ chains. Dotted line is the parabolic fit; $\beta = 1 + 2.5\tau - \tau^2$.

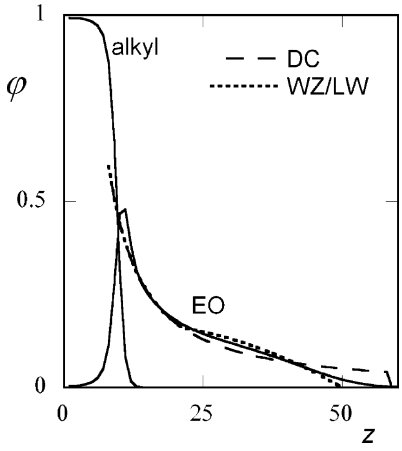


**Figure 5.** Volume fraction profile for a micelle of $C_{20}EO_{200}C_{20}$ chains in a good solvent for the polymer backbone ($\tau = 1$). $z$ is the radial distance to the center in lattice units. The drawn lines are the profiles for the alkyl tails and backbones. Dashed line is the decay predicted by the Daoud−Cotton model (DC); dotted line is the two-zone model predicted by Wijmans−Zhulina and Li−Witten (WZ/LW).

We can now derive the following expression for telechelic chains, using eqs 7 and 8

$$\mathrm{CMC} \propto N_B^{(3/2)\beta+k} \tag{9}$$

For telechelics with $C_{20}$ alkyl tails, under $\theta$ conditions for the polymer backbone, the numerical exponent is found to be 5/2. From eq 9, knowing that for the equivalent mono-functional chains $k = 1$, we find that $\beta = 1$ for $\tau = 0$, as was predicted.[7] In the same way, we can extract the values for $\beta$ from the numerical results for chains in a good solvent, for which the value of $\beta$ was so far unknown. In Figure 4, we have plotted $\beta$ as a function of the excluded volume parameter $\tau$ for molecules with $C_{20}$ tails. We find the following empirical relationship for $0 < \tau < 1$; $\beta = 1 + 2.5\tau - \tau^2$. Similar results are found for all tail lengths examined here (from $C_{12}$ to $C_{30}$). The fact that the penalty associated with loop formation is larger for nonideal chains was already predicted by des Cloizeaux for a single self-avoiding chain.[28]

**Micellar Structure.** Information on the structure of the micelles follows most directly from the density profiles of the various segments. In Figure 5, the volume fraction profiles are shown for the core (alkyl) and corona (EO) segments of a $C_{20}$-$(EO)_{200}C_{20}$ micelle in a good solvent for the polymer backbone ($\tau = 1$) at the CMC.

The volume fraction of alkyl tails in the core is almost 1, as can be expected for these types of micellar cores in the strong seggregation limit. The strong decay of the tails in the $z$ direction indicates a sharp interface between the core and the surroundings. We see a peak in $\varphi_{EO}$ at the surface of the hydrophobic core, indicating adsorption of the coronal segments onto the core/solvent interface to shield the core from the solvent. This effect is however not taken into account in the models that will be discussed below.

In their model for the conformations of a star-shaped polymer, Daoud and Cotton (DC)[13] predict a density decay in the radial direction, starting from the center of the star, that goes with either $z^{-1}$ for $\theta$ conditions and $z^{-4/3}$ for chains with excluded volume interactions. For a flowerlike micelle consisting of telechelic polymers, in a good solvent for the polymer backbones, we compare the DC model to our numerical results (dashed line in Figure 5). We see that the DC-regime is only found in the first few lattice layers outward from the core, after which the volume fraction of the coronal chains follows a parabola-like profile.

Wijmans and Zhulina[11] and Li and Witten[10] have described the structure of spherical brushes using a two-zone profile. These models consist of an exclusion zone close to the core where the chain ends cannot penetrate (the so-called *dead-zone*[29]), where DC behavior prevails, which is complemented by an outer zone that the chain ends can freely access. Hence, they derive the following description for the density decay in a spherical brush of swollen chains,[10] adjusted for a micelle with finite core size, $r_{core}$:

$$\varphi_{EO}(z) = \begin{cases} \left(\dfrac{z + r_{core}}{r_{excl}}\right)^{-4/3} \varphi_{EO}(r_{excl}) & \forall \ (z + r_{core}) < r_{excl} \\ \dfrac{11B}{2\nu}(h^{*2} - (z + r_{core})^2) & \forall \ r_{excl} < (z + r_{core}) < r \end{cases} \tag{10}$$

where $\varphi_{EO}$ is the volume fraction of coronal chains (here EO), $r_{excl} = 0.86(n_{agg}N_B^3a^2\nu)^{1/5}$ is the radius of the exclusion zone, $h^*$ is a height given by the size of the exclusion zone $r_{excl}/h^* = 0.94$, and $r$ is the radius of micelle. $B$ is given by $9/(25N_B^2a^2)$, where $a$ is the Kuhn length (in this lattice model, $a = 1$) and $\nu$ is the swelling exponent ($\nu = 3/5$ for chains in a good solvent).

In Figure 5, we compare this model with a typical SCF result for the density decay in the corona of the flowerlike micelles and see that this addition to the Daoud−Cotton model significantly improves the agreement with our numerical result. This implicates that the models for the structure of spherical brushes can also be used to predict the structure of micelles assembled from telechelic chains and that the formation of loops does not significantly affect the micellar structure.

Self-consistent field theory is ideally suited to study self-assembly as each chain interacts with many neighbors in the crowded environment of the micelle. It is possible that in the dilute outer regions of the corona the self-consistent field prediction is not very accurate.

**Aggregation Number.** In the following, the aggregation number ($n_{agg}$) is defined as the number of hydrophobic tails in the micellar core. The aggregation numbers are calculated at $\Omega = 0$, meaning that we neglect translational entropy of the micelles. In other words, we are calculating the aggregation number at concentrations $\gg$ CMC. In this setup, we consider a fixed total amount of material in micelles, hence an increase in aggregation number results in an equivalent decrease in the number of micelles.

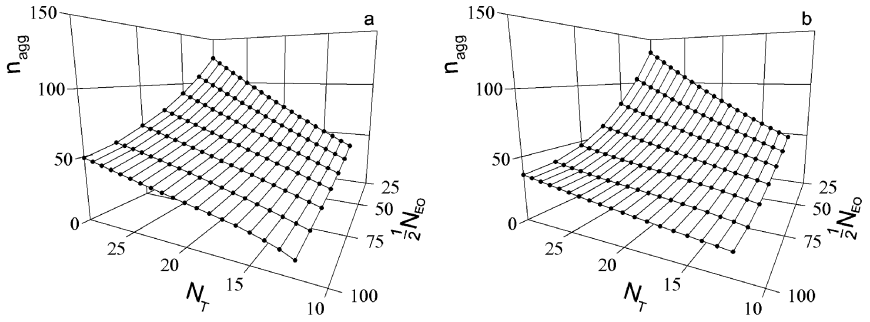


**Figure 6.** Aggregation numbers at $\Omega = 0$ for a mono-functional polymeric surfactant of type $C_{N_T}EO_{(1/2)N_{EO}}$ (a) and a telechelic associative polymer of type $C_{N_T}EO_{N_{EO}}C_{N_T}$ (b) under $\theta$ conditions for the polymer backbone ($\tau = 0$).

In Figure 6, we show the calculated aggregation numbers as a function of $N_{EO}$ and $N_T$ under $\theta$ conditions for the backbone. We see that there are no large differences between the aggregation numbers of the mono-functional chains (Figure 6a) and the telechelic chains (Figure 6b). Unlike the case for the CMC, loop formation does not influence the results here. Because the total number of chains in micelles is fixed, we do not take into account the free energy change associated with transfer of a unimer into a micellee but only look at the most favorable distribution of a given number of chains over a variable number of micelles. We therefore do not see the influence of loop formation, as the entropy loss per chain due to loop formation is independent of the size of the micelle.

The decrease of the aggregation number with $N_{EO}$ is the result of increasing elastic stress on the coronal chains with increasing backbone length. The increase in aggregation number with $N_T$ results from geometrical effects of packing the tails in the core.

The Daoud−Cotton model, which we have introduced above, is based on the stacking of stretching blobs, each containing an equal amount of elastic energy, in concentric layers around the grafting center. The number of blobs per layer is constant and equals the number of arms in the polymer star *f*. The size of the blobs increases with increasing distance from the center. In this way, they account for the fact that stretching is strongest in proximity of the grafting center. In our micellar approach, the aggregation number $n_{agg}$ is equivalent to the number of arms *f*.

The size of a blob follows from geometric considerations

$$\xi(z) = \frac{z}{f^{1/2}} = \frac{z}{n_{agg}^{1/2}} \tag{11}$$

where *z* is the radial distance from the center of the coordinate system. We can obtain the free energy of stretching of the coronal chains, in an approach similar to Halperin,[30] by integrating the osmotic pressure in the corona over the total corona volume. The osmotic pressure $\Pi$ is given by $1/\xi^3$. The free energy of stretching ($F^s$) is given by

$$F^s = \int \Pi \, dV_{corona} = 4\pi \int_{r_{core}}^{r} \frac{z^2}{\xi^3} dz \tag{12}$$

The radius of the core $r_{core}$ equals the cubed root of the dimensionless volume of the core. By assuming that the volume fraction of alkyl tails in the core is unity, we find that

$$r_{core} = n_{agg}^{1/3} N_T^{1/3} \tag{13}$$

In the Daoud−Cotton model, the radius of the star-polymer is given by $N_B^{\nu} n_{agg}^{b}$, where $\nu = 1/2$ and $b = 1/4$ for $\theta$ conditions and $\nu = 3/5$ and $b = 1/5$ for chains in a good solvent. To apply this DC argument to predict the size of the micelle, we must account for the finite volume of the micellar core. We can do this by extending the actual backbone with a number of virtual backbone segments, $N_B^*$, that together correct for the size of the core, such that $r_{core} = n_{agg}^{1/3} N_T^{1/3} = (N_B^*)^{\nu} n_{agg}^{b}$. Rewriting gives $N_B^* = (n_{agg}^{(1/3)-b} N_T^{1/3})^{1/\nu}$. With this correction, the size of the micelle is given by

$$r = (N_B + N_B^*)^{\nu} n_{agg}^{b} \tag{14}$$

Inserting these expressions and the blob size, as defined in eq 11, into eq 12 gives

$$F^s \propto \int_{r_{core}}^{r} \left(\frac{n_{agg}^{1/2}}{z}\right)^3 z^2 \, dz = n_{agg}^{3/2} \ln\left[\frac{(N_B + N_B^*)^{\nu} n_{agg}^{b-(1/3)}}{N_T^{1/3}}\right] \tag{15}$$

As a first-order approximation we can balance this elastic energy in the corona with the excess free energy at the interface of the hydrophobic core and its surroundings ($F^{\sigma}$) to obtain $n_{agg}$.

Although the micellar core cannot be considered as a homogeneous macroscopic phase, we assume that there is some sort of interfacial tension $\gamma$ between the core and its surroundings. If we assume that $\gamma$ is a constant, the excess free energy of the interface then follows

$$F^{\sigma} = \gamma A_{core} \propto n_{agg}^{2/3} N_T^{2/3} \tag{16}$$

where the surface area of the spherical core is given by $A_{core} = (n_{agg} N_T)^{2/3}$. By balancing

$$\frac{\partial F^s}{\partial n_{agg}} = \frac{-\partial F^{\sigma}}{\partial n_{agg}} \tag{17}$$

and inserting the exponents $\nu$ and *b* as given above, we find the following result

$$n_{agg}^{-5/6} \propto f(N_T, N_B, n_{agg}) = \begin{cases} N_T^{-2/3} \ln \dfrac{(N_B + N_B^*)^{1/2} n_{agg}^{-1/12}}{N_T^{1/3}} & \forall \ \tau = 0 \\ N_T^{-2/3} \ln \dfrac{(N_B + N_B^*)^{3/5} n_{agg}^{-2/15}}{N_T^{1/3}} & \forall \ \tau > 0 \end{cases} \tag{18}$$

where

$$N_B^* = \begin{cases} n_{agg}^{1/6} N_T^{2/3} & \forall \ \tau = 0 \\ n_{agg}^{4/15} N_T^{2/3} & \forall \ \tau > 0 \end{cases} \tag{19}$$

The agreement between the model and the numerical results is found to be very satisfying for both the $N_T$- and the

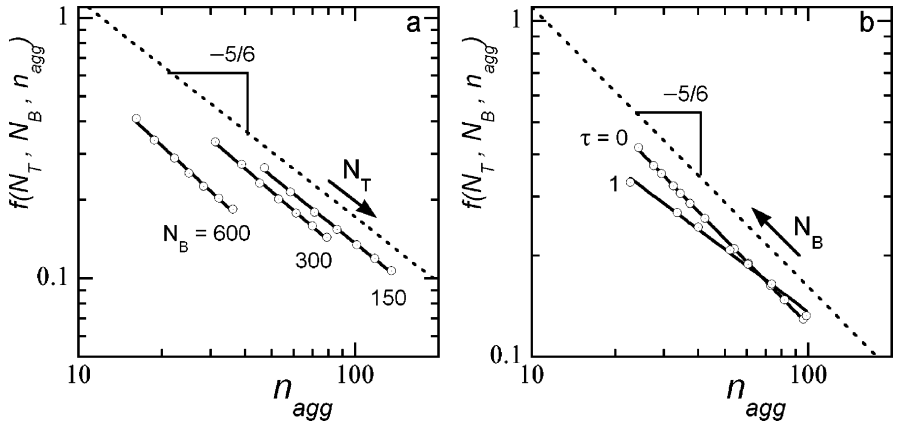


**Figure 7.** Comparison of the numerically calculated aggregation numbers and the scaling model in eq 18. Open symbols are numerical results, solid lines are corresponding power-law fits, and dotted lines indicate the exponent of −5/6, as predicted by eq 18. (a) For fixed values of $N_B$ (600, 300, and 150) as a function of alkyl length $N_T$, which increases in the direction of the arrow, under $\theta$ conditions for the polymer backbone and (b) for $N_T = 20$ as a function of backbone length $N_B$, which increases in the direction of the arrow, for $\theta$ ($\tau = 0$) and good solvent conditions ($\tau = 1$) for the polymer backbone.

$N_B$-dependence of $n_{agg}$, as shown in Figure 7a, b. Upon varying the alkyl chain length, for fixed values of $N_B$ under $\theta$ conditions for the polymer backbone, the numerical results give a slope that is equal or close to the predicted slope (on double logarithmic scale) of −5/6 (Figure 7a). This indicates that even for the smallest backbone length considered here ($N_{EO} = 50$) the micelles can be seen as star-like structures and are not yet in the crewcut regime.

When we change the backbone length under $\theta$ conditions, for fixed $N_T$, we also find a good agreement between the model and SCF results (Figure 7b). However, if we do the same under good solvent conditions for the backbone, the agreement is significantly less. We attribute this to the fact that the value 3/5 for the swelling exponent $\nu$ is valid in the limit of infinite chain lengths and might not be accurate for the finite chain lengths chosen here.

In this paper, our interest is in the scaling behavior of the aggregation number, analyzed using the scaling argument above. However, using our numerical results, we can determine the arbitrary prefactor needed to convert the proportionality in eq 18 into an equality. For $\theta$ conditions, where the model describes the numerical scaling best, we find a prefactor of 0.17.

Meng and Russel have recently published a study on the aggregation numbers of telechelic micelles using a similar analytical approach, however using different terms to account for the corona and core contribution to the free energy of micellization,[9] where they focused on a smaller range of somewhat larger polymeric backbones ($N_{EO}$ between 200 and 800). For the tail length dependence, they use $n_{agg} \propto N_T^{4/5}$, which is the same relation used by, e.g., Francois et al.[4] It is easily shown that, by neglecting the logarithmic term, eq 18 returns to this result. Although this is a good approximation and gives reasonable correspondence with our numerical results, we cannot neglect the logarithmic correction to find the exact dependence of the aggregation number on the hydrophobe length. For the dependence of the aggregation number on the backbone length, a significantly different result is presented by Meng and Russel; where we find a logarithmic dependence, they report that $n_{agg} \propto N_B^{-1/5}$. In our SCF calculations, no simple power-law behavior could be seen for the $N_{EO}$ -range investigated.

## Conclusions

We have studied the micellization of telechelic associative polymers and their mono-functional analogues focusing on the proportionality of, e.g., the CMC and the aggregation number on the size of the hydrophilic and hydrophobic block(s). The numerical results from the self-consistent field calculations are compared to approximate, but insightful, scaling arguments. We have shown that the scaling of the CMC with the hydrophilic backbone length could be explained with a simple model based on the entropic penalty for loop formation. We also found that coronal density profiles are reasonably described by the Wijmans−Zhulina and Li−Witten models, which are elaborations on the Daoud−Cotton model that could only describe the coronal density decay in a limited part of the corona. Furthermore, we have shown that the proportionality of the aggregation number with the length of the hydrophobic tail and hydrophilic backbone is well described by an expression based on the same Daoud−Cotton model, taking into account the finite volume of the core. In summary, we conclude that simple scaling arguments can be used to predict the various aspects of the micellization of telechelic associative polymers in reasonable detail.

**Acknowledgment.** The work of J. Sprakel forms part of the research program of the Dutch Polymer Institute (DPI), project #564.

## References and Notes

(1) Xu, B.; Yekta, A.; Winnik, M. A. *Colloids Surf., A* **1996**, *112*, 239.
(2) Pham, Q. T.; Russel, W. B.; Thibeault, J. C.; Lau, W. *Macromolecules* **1999**, *32*, 2996.
(3) Semenov, A. N.; Joanny, J.-F.; Kokhlov, A. R. *Macromolecules* **1995**, *28*, 1066.
(4) Francois, J.; Beaudoin, E.; Borisov, O. *Langmuir* **2003**, *19*, 10011.
(5) Halperin, A. *Europhys. Lett.* **1989**, *8*, 351.
(6) Halperin, A.; Alexander, S. *Macromolecules* **1989**, *22*, 2403.
(7) ten Brinke, G.; Hadziioannou, G. *Macromolecules* **1987**, *20*, 486.
(8) Balsara, N. P.; Tirrel, M.; Lodge, T. P. *Macromolecules* **1991**, *24*, 1975.
(9) Meng, X. X.; Russel, W. B. *Macromolecules* **2005**, *38*, 593.
(10) Li, H.; Witten, T. A. *Macromolecules* **1994**, *27*, 449.
(11) Wijmans, C. M.; Zhulina, E. B. *Macromolecules* **1993**, *26*, 7214.
(12) Dan, N.; Tirrell, M. *Macromolecules* **1992**, *25*, 2890.
(13) Daoud, M.; Cotton, J. P. *J. Phys.* **1982**, *43*, 531.
(14) Fleer, G. J.; Cohen Stuart, M. A.; Scheutjens, J. M. H. M.; Cosgrove, T.; Vincent, B. *Polymers at Interfaces*; Chapman and Hall: London, 1993.

(15) Jodar-Reyes, A. B.; Ortega-Vinuesa, J. L.; Martin-Rodriguez, A.; Leermakers, F. A. M. *Langmuir* **2002**, *18*, 8706.
(16) Lauw, Y.; Leermakers, F. A. M.; Cohen Stuart, M. A.; Borisov, O. V.; Zhulina, E. B. *Macromolecules* **2006**, *16*, 3628.
(17) Hill, T. L. *Thermodynamics of Small Systems, Parts 1 and 2*; Dover Publications Inc.: New York, 1994.
(18) Hall, D. G.; Pethica, B. A. In *Nonionic surfactants*; Schick, M. J., Ed.; Marcel Dekker Inc.: New York, 1967; Chapter 16.
(19) Scheutjens, J. M. H. M.; Fleer, G. J. *J. Phys. Chem.* **1979**, *83*, 1619.
(20) Scheutjens, J. M. H. M.; Fleer, G. J. *J. Phys. Chem.* **1980**, *84*, 178.
(21) Evers, O. A.; Scheutjens, J. M. H. M.; Fleer, G. J. *Macromolecules* **1990**, *23*, 5221.
(22) Jodar-Reyes, A. B.; Leermakers, F. A. M. *J. Phys. Chem. B* **2006**, *110*, 6300.
(23) Flory, P. J. *Principles of Polymer Chemistry*; Cornell University Press: Ithaca, NY, 1953.
(24) de Bruijn, V. G.; van den Broeke, L. J. P.; Leermakers, F. A. M.; Keurentjes, J. T. F. *Langmuir* **2002**, *18*, 10467.
(25) Tanford, C. *The Hydrophobic Effect, Formation of Micelles and Biological Membranes*; Wiley: New York, 1980.
(26) van Os, N. M.; Haak, J. R.; Rupert, L. A. M. *Physico-Chemical Properties of Selected Anionic, Cationic and Nonionic Surfactants*; Elsevier: Amsterdam, 1993.
(27) Jacobson, H.; Stockmayer, W. H. *J. Chem. Phys.* **1950**, *18* (12), 1600.
(28) des Cloizeaux, J. *Phys. Rev. A* **1974**, *10*, 1665.
(29) Semenov, A. N. *Sov. Phys. JETP* **1985**, *61*, 733.
(30) Halperin, A. *Macromolecules* **1987**, *30*, 2943.